

Spectroscopic studies of jet-cooled AlNi

Jane M. Behm, Caleb A. Arrington, and Michael D. Morse
Department of Chemistry, University of Utah, Salt Lake City, Utah 84112

(Received 16 February 1993; accepted 19 July 1993)

Resonant two-photon ionization spectroscopy has been used to interrogate diatomic AlNi produced by laser vaporization of a 1:1 alloy target in a supersonic molecular beam of helium. Although a large density of states in this molecule prohibits a concise elucidation of its electronic structure, the presence of discrete transitions has allowed several bands to be rotationally resolved. From the analysis of these bands the ground state has been determined as $X^2\Delta_{5/2}$, originating from the $3s_{\text{Al}}^2 3d_{\text{Ni}}^9 \sigma^2$ configuration, and the bond length has been measured as 2.3211 ± 0.0007 Å. The dissociation energy and ionization potential of AlNi have also been determined as $D_0^{\circ}(\text{AlNi}) = 2.29 \pm 0.05$ eV and $\text{I.P.}(\text{AlNi}) = 6.95 \pm 0.09$ eV, respectively.

I. INTRODUCTION

The spectroscopic analysis of AlNi has been completed in a continuation of a systematic gas-phase spectroscopic investigation of the transition metal aluminides which has recently been initiated in this laboratory. The aim of this study, as described in more detail in the preceding paper,¹ is to provide fundamental experimental measurements relevant to the chemical bonding between the p -block and d -block metals. Fundamental results obtained in this way may well be relevant to the forces acting between atoms in the bulk alloys of these elements, and this may provide new insights into the metallurgy of aluminum transition metal alloys.

As presented in the preceding paper,¹ the chemical bonding in the ground state of AlCu derives from the interaction of an $3s^2 3p^1$ aluminum atom and a $3d^{10} 4s^1$ copper atom, and occurs via the formation of a σ bond between the $4s$ electron of copper and the lone $3p$ electron of aluminum. This leads to a ground molecular term of $^1\Sigma^+$ for AlCu. In contrast to AlCu, the open $3d$ subshell of nickel leads to many more possibilities for the ground electronic state of AlNi, and contributes to a much greater density of excited electronic states as well. The chemical bonding in AlNi could result from the interaction of either a $3d^8 4s^2$, 3F nickel atom or a $3d^9 4s^1$, 3D nickel atom with the $3s^2 3p^1$, $^2P^{\circ}$ ground state aluminum atom. Both asymptotes lie very low in energy, with the 3D_3 level of the nickel atom lying only 204.8 cm^{-1} above the 3F_4 ground level.² Since the predominant bonding is expected to occur through the same $4s\sigma$ - $3p\sigma$ bonding interaction as occurs in AlCu, the interaction of a $3d^9 4s^1$, 3D nickel atom with aluminum would presumably be most favorable for a $p\sigma$ approach of the aluminum to the nickel atom, leading to a ground electronic state deriving from a $3s_{\text{Al}}^2 3d_{\text{Ni}}^9 ({}^2D)\sigma^2$ configuration. This is analogous to the $3d_{\text{Ni}}^9 ({}^2D) 3d_{\text{Cu}}^{10} \sigma^2$ ground configuration of NiCu,^{3,4} and would lead to ${}^2\Sigma^+$, ${}^2\Pi$, and ${}^2\Delta$ molecular terms, depending on the location of the $3d$ hole on the nickel atom. As in NiCu, the effective positive charge of the aluminum core would be expected to cause these terms to order as ${}^2\Delta < {}^2\Pi < {}^2\Sigma^+$, leading to a ground state of $X^2\Delta_{5/2}$.⁵

On the other hand, the interaction of a $3d^8 4s^2$, 3F

nickel atom with aluminum would presumably be most favorable when the aluminum approaches the nickel atom in a $p\pi$ orientation, since otherwise the total of three σ electrons would lead to a destabilized $3s_{\text{Al}}^2 3d_{\text{Ni}}^8 ({}^3F)\sigma^2 \sigma^{*1}$ state. With the $3p$ electron of aluminum in a π orientation, however, the molecule will possess a $3s_{\text{Al}}^2 3d_{\text{Ni}}^8 ({}^3F)\sigma^2 \pi^1$ electronic configuration, and because of the contracted nature of the $3d$ orbitals in nickel, little interaction between the aluminum $p\pi$ orbital and the $3d$ orbitals of nickel is expected. Thus, the interaction of a $3d^8 4s^2$, 3F nickel atom with aluminum would probably give a high-spin quartet ($S = \frac{3}{2}$) state as its lowest molecular term, since exchange interactions would favor a high-spin coupling of the 3F core on nickel with the π^1 electron.

As has been discussed by Field,⁶ the spherically symmetric B_0^0 term in the ligand field model leads to a preferential stabilization of more diffuse orbitals if the ligand is negatively charged. Thus, if the aluminum atom in AlNi were negatively charged, the $3d^8 4s^2 ({}^3F)$ configuration of nickel would be favored, leading to a high-spin quartet ground state arising from the $3s_{\text{Al}}^2 3d_{\text{Ni}}^8 ({}^3F)\sigma^2 \pi^1$ electronic configuration. On the other hand, the B_0^0 term will lead to a preferential stabilization of more compact orbitals if the ligand is positively charged, thus favoring the $3d^9 4s^1 ({}^3D)$ configuration of nickel if the aluminum atom in AlNi takes on a positive charge. Given the electropositive nature of aluminum, this latter possibility seems most likely, leading to a predicted ground electronic state of $3s_{\text{Al}}^2 3d_{\text{Ni}}^9 ({}^2D)\sigma^2$, ${}^2\Delta_{5/2}$ for AlNi.

In the remainder of this article experimental results are presented that support the assignment of the ground state of AlNi as ${}^2\Delta_{5/2}$, deriving from the $3s_{\text{Al}}^2 3d_{\text{Ni}}^9 ({}^2D)\sigma^2$ electronic configuration. In addition to determining the ground state of AlNi as ${}^2\Delta_{5/2}$, the bond length, bond strength, and ionization potential of the molecule have been determined, and these properties are compared to those of the filled d -subshell analog, AlCu. To our knowledge this represents the first study, spectroscopic or otherwise, to be undertaken on the AlNi diatomic molecule.

Section II describes the experimental methods utilized in this investigation and Sec. III presents the results obtained for AlNi. In Section IV comparisons are made with the closed d -subshell analog, AlCu, and with other related

metal molecules. A brief summary of our results follows in Sec. V.

II. EXPERIMENT

The present spectroscopic investigation of AlNi was performed using an apparatus that is described in detail in the preceding paper.¹ In the present study the metal target used for pulsed laser vaporization was 0.35 cm in thickness and 2.6 cm in diameter, and was prepared by heating an equimolar sample of aluminum and nickel in an electric arc furnace until the component metals melted and were thoroughly mixed by convection. This was then ground flat and subjected to laser vaporization as described in the preceding article on AlCu.¹ The optical spectra of ²⁷Al⁵⁸Ni and ²⁷Al⁶⁰Ni were collected by individually monitoring the ion signals at masses 85 and 87, respectively, as a function of dye laser frequency, using either KrF (248 nm, 5.00 eV) or ArF (193 nm, 6.42 eV) radiation to provide the second photon in a resonant two-photon ionization scheme. For the AlNi studies all of the bands that were rotationally resolved at 0.04 cm⁻¹ resolution fell within the region of the I₂ atlas,⁷ so it was not necessary to employ Raman shifting for accurate absolute calibration of the scans.

III. RESULTS

A. Low resolution spectrum and the bond strength of AlNi

The low resolution (≈ 0.8 cm⁻¹) resonant two-photon ionization (R2PI) spectrum of AlNi was recorded over the entire range from 12 500 to 20 700 cm⁻¹. In the region below 16 000 cm⁻¹ the vibronic bands are relatively sparse, but no regular vibronic progressions are evident. All that can be discerned from this portion of the spectrum are four sets of origin (0-0) and 1-0 vibronic bands, with vibrational intervals ($\Delta G_{1/2}$) of 200 to 250 cm⁻¹. The vibrational numbering of these bands was determined by measuring the shift in band origins between the ²⁷Al⁵⁸Ni and ²⁷Al⁶⁰Ni isotopic modifications. Excited state lifetimes for states accessed in this energy region ranged from 10 to 20 μ s, and attempts to rotationally resolve these bands were unsuccessful due to poor signal enhancement.

At higher energies the spectrum becomes increasingly congested, making attempts to assign vibronic progressions futile. This high degree of vibronic congestion is expected because the open 3*d* subshell of nickel provides a large number of possible angular momentum couplings, leading to many distinct potential energy surfaces. It is a difficult computational task to calculate all of these potential energy curves from first principles, but quite simple to estimate the density of electronic states at the separated atom limit. This may be done by noting that the number of distinct relativistic adiabatic [Hund's case (c)] potential energy curves arising from a given separated atom limit is given by $(2J_{\text{Al}} + 1)(2J_{\text{Ni}} + 1)/2$, where J_{Al} and J_{Ni} are the total angular momentum quantum numbers ($J = L + S$) for the states of the separated aluminum and nickel atoms, respectively. Using the well-known atomic energy levels of aluminum and nickel,² a simple calculation shows that 123

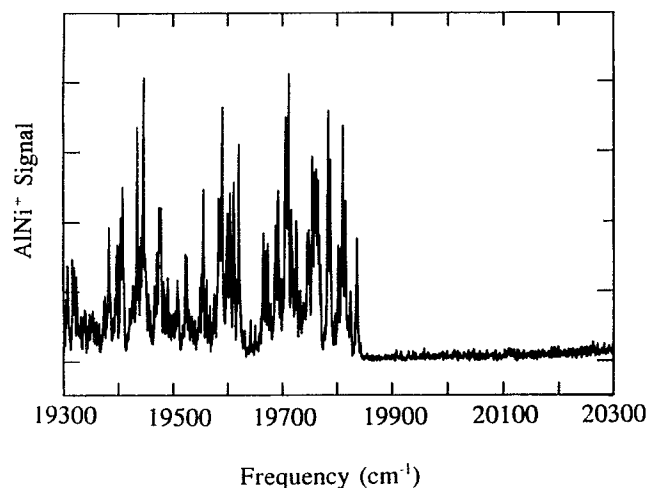


FIG. 1. Predissociation threshold in AlNi, observed by resonant two-photon ionization using a dye laser operating on coumarin 500 laser dye, in conjunction with KrF excimer radiation, which provided the second, ionizing photon. The dense forest of transitions terminates abruptly at 19 836 cm⁻¹, allowing the bond strength of AlNi to be determined as $D_0^{\circ}(\text{AlNi}) = 2.29 \pm 0.05$ eV.

distinct relativistic adiabatic potential curves arise within 3600 cm⁻¹ of the ground separated atom limit. With this density of low-lying potential energy curves, it should come as no surprise that the vibronic spectrum becomes quite congested as one scans to the blue of 16 000 cm⁻¹. While this is not nearly as many states as arise from diatomics composed of two open *d* subshell atoms (such as V₂, which generates 1378 potential energy curves within 3600 cm⁻¹ of the ground state separated atom limit), it nevertheless provides far more states than are found in AlCu (which generates only eight states within the same energy range).

While scanning to the blue in this dense forest of states, an abrupt onset of predissociation was observed at approximately 19 840 cm⁻¹, as displayed in Fig. 1. By converting the dye laser to the high resolution configuration, the predissociation threshold was precisely located at $19\,836 \pm 1$ cm⁻¹ using the well-known absorption spectrum of I₂ for calibration.⁷ Thus a rigorous upper limit of $D_0^{\circ}(\text{AlNi}) \leq 2.459$ eV ($19\,836$ cm⁻¹) is obtained. In previous studies a similar abrupt onset of predissociation in a dense manifold of excited electronic states has been observed in at least 16 different diatomic transition metals.⁸⁻¹³ As has been discussed elsewhere,¹¹ a predissociation threshold may be inferred to correspond to the thermochemical bond strength if: the threshold is sharp and well defined, without evidence of Franck-Condon difficulties in either the excitation or predissociation step; dissociation can occur to the ground separated atom limit while preserving good quantum numbers, such as Ω , g/u , and $0^+/0^-$; and either the ground separated atom limit generates a considerable number of molecular potential energy surfaces, some of which may be predicted to be repulsive, or the ground separated atom limit generates a much larger number of attractive molecular potential energy surfaces,

allowing weaker predissociation processes to dominate by sheer strength of numbers.

The requirement of repulsive curves originating from the lowest separated atom limits was originally invoked to explain the failure of NiPd and PdPt to display a sharp predissociation threshold.^{12,13} On the other hand, the requirement that good quantum numbers such as Ω , g/u , and $0^+/0^-$ be conserved was invoked to explain the existence of a double dissociation threshold in V_2 .^{9,10} In the case of AlNi the expected density of electronic states (123 distinct potential curves arising within 3600 cm^{-1} of the ground separated atom limit) is small enough that both requirements should probably be considered. In AlNi the lowest separated atom limits are $\text{Al}(3s^23p^1, ^2P^\circ) + \text{Ni}(3d^94s^1, ^3D)$ and $\text{Al}(3s^23p^1, ^2P^\circ) + \text{Ni}(3d^84s^2, ^3F)$. The former limit will certainly generate repulsive curves, as the interaction of an aluminum atom in the $3s^23p\sigma^1$ orientation with a $3d^94s^1, ^3D$ nickel atom can yield repulsive states described as $3s_{\text{Al}}^23d_{\text{Ni}}^9(^2D)\sigma^1\sigma^{*1}$ (the $^4\Delta$, $^4\Pi$, and $^4\Sigma^+$ states) in addition to the attractive states described as $3s_{\text{Al}}^23d_{\text{Ni}}^9(^2D)\sigma^2$ (the $^2\Delta$, $^2\Pi$, and $^2\Sigma^+$ states). Although one might think that repulsive $3s_{\text{Al}}^23d_{\text{Ni}}^9(^2D)\sigma^1\sigma^{*1}$, $^2\Delta$, $^2\Pi$, and $^2\Sigma^+$ states would also arise from this limit, all of the states correlating to $\text{Al}(3p\sigma^1, ^2\Sigma^+) + \text{Ni}(3d^94s^1, ^3D)$ have been used up. The repulsive $3s_{\text{Al}}^23d_{\text{Ni}}^9(^2D)\sigma^1\sigma^{*1}$, $^2\Delta$, $^2\Pi$, and $^2\Sigma^+$ states corresponding to a $^3\Sigma^+$ coupling of the $\sigma^1\sigma^{*1}$ framework instead correlate to the $\text{Al}(3p\sigma^1, ^2\Sigma^+) + \text{Ni}(3d^94s^1, ^1D)$ limit, lying some 3400 cm^{-1} above ground state atoms.² Even higher lying are the repulsive $3s_{\text{Al}}^23d_{\text{Ni}}^9(^2D)\sigma^1\sigma^{*1}$, $^2\Delta$, $^2\Pi$, and $^2\Sigma^+$ states that correspond to a $^1\Sigma^+$ coupling of the $\sigma^1\sigma^{*1}$ framework, as these correlate to the ion pair limit $\text{Al}^+(3s^2, ^1S) + \text{Ni}^-(3d^94s^2, ^2D)$.

On the other hand, states deriving from the interaction of an aluminum atom in the $3s^23p\pi^1$ orientation with a $3d^94s^1, ^3D$ nickel atom are expected to be attractive, properly described as $3s_{\text{Al}}^23d_{\text{Ni}}^9(^2D)\sigma^1\pi^1$ states, and having a bond order of at least $\frac{1}{2}$. Finally, the states generated from the $\text{Al}(3s^23p^1, ^2P^\circ) + \text{Ni}(3d^84s^2, ^3F)$ limit must necessarily be attractive, since they correspond to either $3s_{\text{Al}}^23d_{\text{Ni}}^8(^3F)\sigma^2\sigma^{*1}$ or $3s_{\text{Al}}^23d_{\text{Ni}}^8(^3F)\sigma^2\pi^1$ states which also possess a bond order of at least $\frac{1}{2}$. Thus the only molecular states arising from these separated atom limits that must necessarily be repulsive are the $3s_{\text{Al}}^23d_{\text{Ni}}^9(^2D)\sigma^1\sigma^{*1}$, $^4\Lambda$ states that correlate to $\text{Al}(3s^23p^1, ^2P^\circ) + \text{Ni}(3d^94s^1, ^3D)$. Moreover, one would expect the attractive $3s_{\text{Al}}^23d_{\text{Ni}}^9(^2D)\sigma^2$, $^2\Lambda$ and $3s_{\text{Al}}^23d_{\text{Ni}}^9(^2D)\sigma^1\pi^1$ states to correlate to the lower spin-orbit components of the $\text{Al}(3s^23p^1, ^2P^\circ) + \text{Ni}(3d^94s^1, ^3D)$ limit. It is therefore a simple matter of correlating the Ω states out to the separated atom limit, subject to the noncrossing rule, to determine the lowest of the $\text{Al}(3s^23p^1, ^2P_j^\circ) + \text{Ni}(3d^94s^1, ^3D_j)$ limits to generate repulsive states of a given Ω . In this way one may show that the lowest limit to generate repulsive $\Omega = \frac{1}{2}$ or $\frac{3}{2}$ states is $\text{Al}(3s^23p^1, ^2P_{1/2}^\circ) + \text{Ni}(3d^94s^1, ^3D_1)$, 1713.080 cm^{-1} above ground state atoms,² while the lowest limit to generate repulsive $\Omega = \frac{5}{2}$ or $\frac{7}{2}$ states is $\text{Al}(3s^23p^1, ^2P_{3/2}^\circ) + \text{Ni}(3d^94s^1, ^3D_2)$, 991.353 cm^{-1} above ground state atoms.² Thus, although the predissociation threshold at 2.459 eV ($19\,836\text{ cm}^{-1}$) provides a rigorous upper limit on

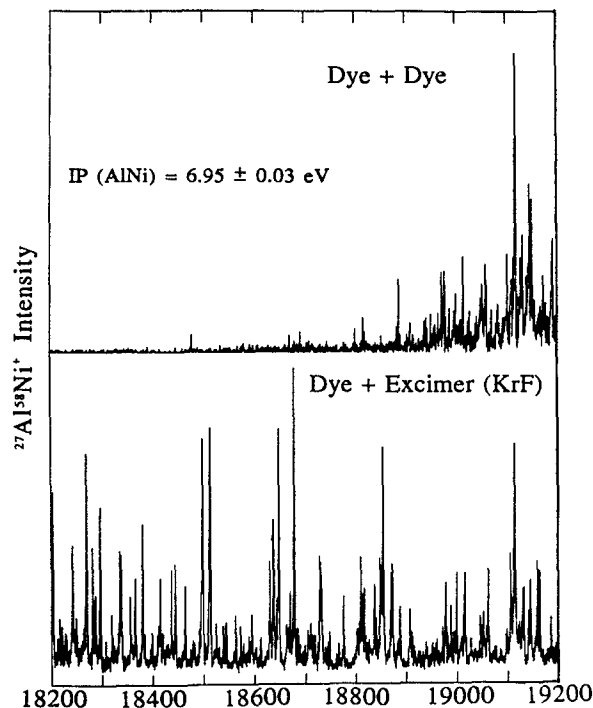


FIG. 2. Determination of the ionization threshold of AlNi. In the upper scan frequency-doubled dye light is employed as the ionization photon in the R2PI scheme. The lower spectrum is obtained using KrF excimer radiation (248 nm, 5.00 eV) as the ionization photon. The last band definitely observed using the frequency-doubled dye light occurs at $18\,670\text{ cm}^{-1}$, placing the ionization potential of AlNi at $6.95 \pm 0.09\text{ eV}$. Both spectra were obtained using coumarin 500 and 540 Å laser dyes to generate the resonant photon in the R2PI process.

$D_0^\circ(\text{AlNi})$, the bond strength of AlNi probably corresponds to this value less 1713 or 991 cm^{-1} . This places the bond strength of AlNi at 2.247 or 2.336 eV , respectively. Accordingly, we recommend a value of $D_0^\circ(\text{AlNi}) = 2.29 \pm 0.05\text{ eV}$, and can state with certainty that $D_0^\circ(\text{AlNi}) \leq 2.459\text{ eV}$.

B. The ionization potential of AlNi

In the resonant two-photon ionization process the first photon comes from a scanning dye laser and is used to excite the molecule, while the second photon is generated by a fixed-frequency excimer laser and is selected so that it is capable of photoionizing the excited state which is produced by absorption of the first photon. An alternate method, however, is to use the fundamental radiation of the dye laser to excite the molecule and the second harmonic of this radiation to provide the second, ionization photon. In either case the sum of the two photon energies must be sufficient to ionize the molecule or no ion signal will be observed. By performing scans over the congested spectrum of AlNi in both configurations it is possible to determine the ionization potential, since as one moves to lower frequencies it will eventually become impossible to ionize the molecule with one scheme or the other.

The results of such an experiment are exhibited in Fig. 2. The lower panel displays the spectrum obtained using

KrF excimer radiation to provide the second photon in the R2PI process, while the upper panel shows the spectrum obtained using the second harmonic of the dye laser for this purpose. At the high frequency end of Fig. 2 both techniques give similar spectra. As one moves to lower frequencies, however, the signal resulting from the dye plus doubled dye R2PI process weakens and eventually disappears. The ionization threshold determined by this method is not extremely sharp, which may be evidence for Franck-Condon problems in the ionization step or for a population of vibrationally excited ($v=1$) molecules in the molecular beam. Nevertheless, it is possible to place the ionization threshold in the range of $18\,650 \pm 250\text{ cm}^{-1}$ in the dye laser fundamental. This places the total energy required for ionization at $55\,950 \pm 750\text{ cm}^{-1}$, which may be corrected for the expected field ionization shift of the ionization potential to give $\text{I.P.}(\text{AlNi}) = 56\,025 \pm 750\text{ cm}^{-1}$, or $\text{I.P.}(\text{AlNi}) = 6.95 \pm 0.09\text{ eV}$.

Having experimentally determined both the bond strength and the ionization potential of AlNi, the bond strength of the cation AlNi^+ can easily be determined by referencing the atomic ionization potentials of Al (5.985 77 eV) (Ref. 14) and Ni (7.637 eV) (Ref. 15) and by completing the appropriate thermodynamic cycles:

$$D_0^\circ(\text{Al}^+-\text{Ni}) = D_0^\circ(\text{Al}-\text{Ni}) + \text{I.P.}(\text{Al}) - \text{I.P.}(\text{AlNi}) \quad (3.1)$$

and

$$D_0^\circ(\text{Al}-\text{Ni}^+) = D_0^\circ(\text{Al}-\text{Ni}) + \text{I.P.}(\text{Ni}) - \text{I.P.}(\text{AlNi}), \quad (3.2)$$

thereby providing $D_0^\circ(\text{Al}^+-\text{Ni}) = 1.33 \pm 0.10\text{ eV}$ and $D_0^\circ(\text{Al}-\text{Ni}^+) = 2.98 \pm 0.10\text{ eV}$.

C. Rotationally resolved spectra of AlNi

The high density of vibronic states in AlNi allows an abrupt predissociation threshold to be observed, but precludes the assignment of vibrational progressions within the various excited electronic states. Nevertheless, the density of vibronic states is still sufficiently sparse that isolated single bands may be found. Although one cannot readily unravel the excited states of this molecule, rotationally resolved spectroscopy on these isolated bands can provide important information about the ground state. With this in mind high resolution scans (0.04 cm^{-1}) were performed on four vibronic bands of AlNi.

Absolute line positions are provided in Table I, as calibrated using the I_2 atlas⁷ and corrected for the Doppler shift experienced by the AlNi molecules as they move toward the radiation source at the beam velocity of helium ($1.77 \times 10^5\text{ cm/s}$). This minor correction amounted to approximately 0.106 cm^{-1} in this range of frequencies. Figure 3 presents one of these rotationally resolved spectra for the predominant isotopic modification, $^{27}\text{Al}^{58}\text{Ni}$. The bandhead in the *R* branch indicates that the Al-Ni bond lengthens upon electronic excitation. In addition, the presence of strong *R* and *P* branches and a *Q* branch which rapidly diminishes in intensity with increasing *J* is characteristic of parallel bands ($\Delta\Lambda=0$ and $\Delta\Omega=0$).¹⁶ With this

in mind, possible assignments of $\Omega'=\frac{1}{2}\leftarrow\Omega''=\frac{1}{2}$, $\Omega'=\frac{3}{2}\leftarrow\Omega''=\frac{3}{2}$, and $\Omega'=\frac{5}{2}\leftarrow\Omega''=\frac{5}{2}$ were considered. The clear observation of the first lines *P*(3.5) and *Q*(2.5) showed that the band could be assigned as $\Omega'=\frac{5}{2}\leftarrow\Omega''=\frac{5}{2}$. Following this assignment a least squares fit of the line positions to the standard formula

$$\nu = \nu_0 + B'J'(J'+1) - B''J''(J''+1) \quad (3.3)$$

confirmed the transition as $\Omega'=\frac{5}{2}\leftarrow\Omega''=\frac{5}{2}$, and allowed accurate values of ν_0 , B_0'' , and B' to be obtained.

Similar analyses were performed for the remaining three bands, which included an $\Omega'=\frac{3}{2}\leftarrow\Omega''=\frac{5}{2}$ band at $17\,761.626\text{ cm}^{-1}$, an $\Omega'=\frac{7}{2}\leftarrow\Omega''=\frac{5}{2}$ band at $18\,075.772\text{ cm}^{-1}$, and an $\Omega'=\frac{7}{2}\leftarrow\Omega''=\frac{5}{2}$ band at $18\,143.147\text{ cm}^{-1}$. The fitted parameters are listed in Table I along with their 1σ error limits. The four independent measurements of B_0'' were combined to obtain $B_0'' = 0.169\,98 \pm 0.000\,10\text{ cm}^{-1}$, from which $r_0'' = 2.3211 \pm 0.0007\text{ \AA}$ is derived (uncertainties represent 1σ error limits).

IV. DISCUSSION

Apart from Bondybey's ground breaking work on AlCu (Ref. 17) the present investigation of AlNi and the preceding paper on AlCu (Ref. 1) represent the first gas phase spectroscopic studies of the $3d$ series transition metal aluminides. The results of these studies show AlCu and AlNi to be quite similar in bond length (2.3389 ± 0.004 vs $2.3211 \pm 0.0007\text{ \AA}$), bond strength (2.315 ± 0.012 vs $2.29 \pm 0.05\text{ eV}$), ionization potential (7.065 ± 0.014 vs $6.95 \pm 0.09\text{ eV}$), and cationic bond strength (1.236 ± 0.018 vs $1.33 \pm 0.10\text{ eV}$). These results provide strong evidence that the chemical bonding is similar in both species (particularly as neutrals). Since the only reasonable candidate for the ground $^1\Sigma^+$ state of AlCu is the $3s_{\text{Al}}^2 3d_{\text{Cu}}^{10} \sigma^2$ configuration which results from an $s\sigma_{\text{Cu}} - p\sigma_{\text{Al}}$ two electron bond, the ground state of AlNi is assigned as deriving from the analogous $3s_{\text{Al}}^2 3d_{\text{Ni}}^9 \sigma^2$ configuration. The observed ground state value of $\Omega=\frac{5}{2}$ then must correspond to the $^2\Delta_{5/2}$ state, which is the only state deriving from the $3s_{\text{Al}}^2 3d_{\text{Ni}}^9 \sigma^2$ configuration with $\Omega=\frac{5}{2}$. Furthermore, it is predicted by a ligand field model to be the lowest level deriving from this configuration.⁵ Using the methods presently available in our group it could not be determined whether the energetics of the remaining states of the $3s_{\text{Al}}^2 3d_{\text{Ni}}^9 \sigma^2$ manifold are accurately predicted by the ligand field model.⁵ Further work involving either dispersed fluorescence or stimulated emission pumping will be required to clarify this issue.

The similarities in electronic structure that are found in AlNi and AlCu do not persist so strongly in the cations AlNi^+ and AlCu^+ , however. As discussed in the preceding article,¹ the ground state of AlCu^+ is either $3s_{\text{Al}}^2 3d_{\text{Cu}}^{10} \sigma^1$, $^2\Sigma^+$, where the presence of only one σ bonding electron reduces the bond strength of AlCu^+ as compared to AlCu, or (more likely) $3s_{\text{Al}}^2 3d_{\text{Cu}}^9 \sigma^2$, where the promotion energy required to excite the copper atom to the $3d^9 4s^2$ state lowers the bond strength considerably. This is similar to the situation in CuH^+ and CuH, where CuH^+ is bound by only $0.92 \pm 0.13\text{ eV}$,¹⁸ while CuH is bound by 2.65 ± 0.17

TABLE I. Rotationally resolved bands of $^{27}\text{Al}^{58}\text{Ni}$ and $^{27}\text{Al}^{60}\text{Ni}$. All line positions are given in wave numbers (cm^{-1}), calibrated using the absorption spectrum of I_2 as described in the text. A correction was also applied to account for the Doppler shift experienced by the AlNi molecules as they traveled toward the radiation source at the beam velocity of helium ($1.77 \times 10^5 \text{ cm/sec}$). Residuals in the least-squares fit of the line positions to $\nu = \nu_0 + B'J'(J'+1) - B''J''(J''+1)$ are given in units of 0.001 cm^{-1} following each entry in parentheses.

Rotational Line	17762 cm^{-1} Band ^a $\Omega' = 3/2 \leftarrow \Omega'' = 5/2$		18076 cm^{-1} Band ^a $\Omega' = 7/2 \leftarrow \Omega'' = 5/2$		18147 cm^{-1} band ^a $\Omega' = 7/2 \leftarrow \Omega'' = 5/2$	18265 cm^{-1} band ^a $\Omega' = 5/2 \leftarrow \Omega'' = 5/2$	
	$^{27}\text{Al}^{58}\text{Ni}$	$^{27}\text{Al}^{60}\text{Ni}$	$^{27}\text{Al}^{58}\text{Ni}$	$^{27}\text{Al}^{60}\text{Ni}$	$^{27}\text{Al}^{58}\text{Ni}$	$^{27}\text{Al}^{58}\text{Ni}$	$^{27}\text{Al}^{60}\text{Ni}$
P(10.5)						18258.308(-5)	
P(9.5)		17756.936(-8)				18259.153(-2)	
P(8.5)	17757.750(-7)	17757.531(6)	18070.162(-2)	18066.773(0)		18259.943(-1)	18258.156(-1)
P(7.5)	17758.296(-30)	17758.074(-4)	18071.167(-2)	18067.750(9)		18260.690(10)	18258.934(-6)
P(6.5)	17758.884(19)	17758.594(-8)	18072.083(-3)			18261.369(5)	18259.668(4)
P(5.5)	17759.382(8)	17759.107(9)		18069.436(11)		18261.988(-6)	18260.326(-2)
P(4.5)	17759.850(-2)	17759.561(-4)		18070.137(-3)		18262.563(-9)	18260.932(0)
P(3.5)	17760.308(9)	17760.018(14)	Missing	Missing	Missing	18263.090(-7)	18261.477(0)
P(2.5)	17760.715(-2)	17760.410(-3)	Missing	Missing	Missing	Missing	Missing
Q(10.5)			18070.519(-8)				
Q(9.5)			18071.458(0)	18068.121(-2)		18261.884(4)	
Q(8.5)	17760.417(19)		18072.307(7)	18068.920(-2)		18262.386(4)	
Q(7.5)			18073.059(5)	18069.635(-2)	18144.689(3)	18262.827(-5)	18261.018(2)
Q(6.5)	17760.875(-10)		18073.734(15)	18070.256(-12)	18145.322(1)	18263.237(9)	
Q(5.5)	17761.091(9)	17760.803(2)	18074.288(-8)	18070.809(-6)	18145.877(5)	18263.583(11)	18261.859(9)
Q(4.5)	17761.253(3)	17760.963(5)	18074.792(8)	18071.273(-5)	18146.336(-3)	18263.868(5)	18262.184(6)
Q(3.5)	17761.391(4)	17761.086(-1)	18075.187(4)	18071.652(-5)	18146.711(-9)	18264.097(-4)	18262.447(1)
Q(2.5)	17761.493(0)	17761.188(1)	Missing	Missing	Missing	18264.285(-1)	18262.648(-7)
R(2.5)	17762.576(-5)	17762.285(14)	18076.360(-13)	18072.832(-4)	18147.908(-2)	18265.284(-6)	18263.623(-1)
R(3.5)	17762.772(-13)	17762.482(2)	18076.310(-4)	18072.809(15)	18147.871(3)	18265.393(1)	
R(4.5)	17762.961(2)	17762.641(-20)	18076.166(0)	18072.664(-4)	18147.752(10)	18265.439(-1)	18263.701(0)
R(5.5)	17763.099(-3)	17762.816(3)	18075.929(0)	18072.465(7)	18147.523(-8)		18263.645(-5)
R(6.5)	17763.208(-7)	17762.926(-11)	18075.605(1)	18072.166(2)	18147.250(15)		18263.539(-1)
R(7.5)	17763.302(5)	17763.027(-3)		18071.785(-1)	18146.840(-14)		
R(8.5)				18071.328(4)		18265.119(12)	
R(9.5)						18264.885(-7)	
R(10.5)						18264.616(-8)	
R(11.5)		17763.135(10)					

^aFitted parameters (with 1σ error limits in parentheses): 17 762 cm^{-1} band: $^{27}\text{Al}^{58}\text{Ni}$, $\nu_0 = 17\,761.6264(52)$, $B_0'' = 0.170\,57(29)$, $B' = 0.155\,35(28)$; $^{27}\text{Al}^{60}\text{Ni}$, $\nu_0 = 17\,761.3127(34)$, $B_0'' = 0.169\,12(19)$, $B' = 0.154\,80(17)$. 18 076 cm^{-1} band: $^{27}\text{Al}^{58}\text{Ni}$, $\nu_0 = 18\,075.8811(38)$, $B_0'' = 0.170\,00(20)$, $B' = 0.125\,66(22)$; $^{27}\text{Al}^{60}\text{Ni}$, $\nu_0 = 18\,072.3191(36)$, $B_0'' = 0.168\,48(17)$, $B' = 0.126\,41(17)$. 18 147 cm^{-1} band: $^{27}\text{Al}^{58}\text{Ni}$, $\nu_0 = 18\,147.3878(65)$, $B_0'' = 0.169\,96(50)$, $B' = 0.127\,57(45)$. 18 265 cm^{-1} band: $^{27}\text{Al}^{58}\text{Ni}$, $\nu_0 = 18\,264.5171(26)$, $B_0'' = 0.169\,86(13)$, $B' = 0.143\,43(12)$; $^{27}\text{Al}^{60}\text{Ni}$, $\nu_0 = 18\,262.9152(24)$, $B_0'' = 0.168\,21(12)$, $B' = 0.138\,42(13)$.

eV.¹⁹ In AlNi^+ , however, bonding can result from the interaction of a ground state Al^+ ion ($3s^2, ^1S_0$) and a ground state Ni atom ($3d^8 4s^2, ^3F_4$), leading to a two-electron ps - sd bond and an electron configuration of $3s_{\text{Al}}^2 3d_{\text{Ni}}^8 (^3F)\sigma^2$. Since the ground states of the separated fragments are perfectly set up for donation of the $4s^2$ electrons of nickel into the empty $3p\sigma$ orbital of aluminum, it is somewhat surprising that the bond strength of AlNi^+ is not greater than the measured value of 1.33 ± 0.10 eV.

Although the lack of obvious regular vibronic progressions makes it difficult to characterize the excited states accessed in this study, some general conclusions can be drawn. The fluorescence lifetimes of three of the four states which were rotationally analyzed were measured and found to lie in the range of 6–9 μs . If the only decay process is fluorescence to the ground electronic state, such lifetimes correspond to absorption oscillator strengths of $f \approx 6 \times 10^{-4}$. Taking into account the possibility of fluorescence to other low-lying electronic states in AlNi, it would be more prudent to consider the true absorption oscillator strengths to be below 3×10^{-4} . These values are

similar to the oscillator strengths found for the various $d_{\text{Ni}}^8 (^3F)d_{\text{Cu}}^{10}\sigma^2\sigma^*1$, $^2\Lambda \leftarrow d_{\text{Ni}}^9 d_{\text{Cu}}^{10}\sigma^2$, $X^2\Delta_{5/2}$ band systems of NiCu ($f < 1 \times 10^{-3}$),³ where it was rationalized that the forbidden character of the $3d^8 4s^2 (^3F) \leftarrow 3d^9 4s^1 (^3D)$ transition on the nickel atom (a $g \leftarrow g$ transition) carries over into the molecule, where the reduction in symmetry makes the corresponding transitions weakly allowed. In the case of AlNi, possible upper states of the observed transitions include the states of the $3s_{\text{Al}}^2 3d_{\text{Ni}}^8 (^3F)\sigma^2\sigma^*1$, $3s_{\text{Al}}^2 3d_{\text{Ni}}^8 (^3F)\sigma^2\pi^1$, and $3s_{\text{Al}}^2 3d_{\text{Ni}}^9 (^2D)\sigma^1\pi^1$ manifolds. The long fluorescence lifetime and significant increase in bond length upon electronic excitation ($\Delta r = 0.11$ – 0.38 Å) would suggest that the upper states rotationally analyzed in this study may belong to the $3s_{\text{Al}}^2 3d_{\text{Ni}}^8 (^3F)\sigma^2\sigma^*1$ manifold, although this is very speculative.

It is interesting to note that the ground state bond lengths of Cu_2 (2.2197 Å),²⁰ NiCu (2.2346 ± 0.0005 Å),⁴ Ni_2 (2.200 ± 0.007 Å),⁸ AlCu (2.3389 ± 0.0004 Å),¹ and AlNi (2.3211 ± 0.0007 Å) form a consistent set, in which it is possible to define covalent bond radii for Cu, Ni, and Al as 1.110 Å, 1.100 Å, and 1.223 Å, respectively, which may

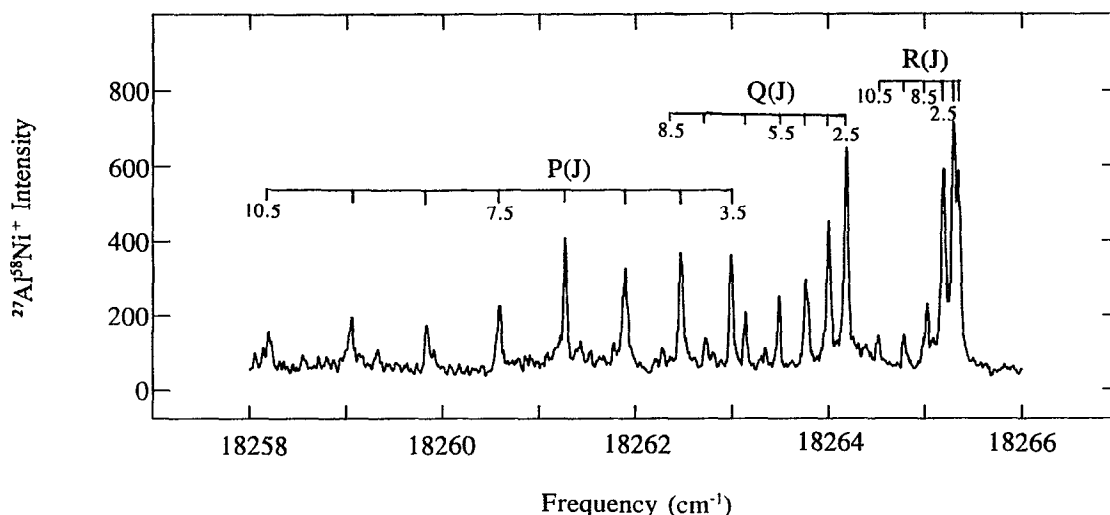


FIG. 3. High-resolution scan over the $\Omega' = \frac{5}{2} \leftarrow X^2\Delta_{5/2}$ band of $^{27}\text{Al}^{58}\text{Ni}^+$ located at $18\,264.517\text{ cm}^{-1}$.

then be combined to reproduce all of the measured bond lengths to an accuracy of 0.02 \AA . This strongly supports the notion that the bonding is similar in these molecules, dominated by $\sigma\text{-}\sigma$ bonds in the transition metal diatomics and by $\sigma\text{-}p\sigma$ bonds in the transition metal aluminides.

Lastly, a comparison of bond strengths shows that the heteronuclear species AlNi is much more strongly bound than either of its homonuclear parents, with $D_0^\circ(\text{Al}_2) = 1.34\text{ eV}$,²¹ $D_0^\circ(\text{Ni}_2) = 2.07\text{ eV}$,⁸ and $D_0^\circ(\text{AlNi}) = 2.29 \pm 0.05\text{ eV}$. Similar results are obtained when comparing Al₂ with Cu₂ ($D_0^\circ = 2.03 \pm 0.02\text{ eV}$) (Ref. 13) and AlCu ($D_0^\circ = 2.315 \pm 0.012\text{ eV}$) (Ref. 1). These trends in bond strength are consistent with the possibility of significant ion-pair character in the AlCu and AlNi ground states, since ionic contributions tend to cause bond strengths to increase.

V. CONCLUSION

A resonant two-photon ionization spectroscopic investigation of AlNi has identified the ground state of the molecule as a $^2\Delta_{5/2}$ state deriving from the $3s^2_{\text{Al}}3d^9_{\text{Ni}}\sigma^2$ manifold. The observation of a predissociation threshold in a dense vibronic spectrum has led to a measured value for the bond strength of $D_0^\circ(\text{AlNi}) = 2.29 \pm 0.05\text{ eV}$, and a comparison of the R2PI spectra obtained using two different ionization schemes has allowed the ionization potential to be determined as $\text{I.P.}(\text{AlNi}) = 6.95 \pm 0.09\text{ eV}$. These values may be combined to provide the cationic bond strength, $D_0^\circ(\text{Al}^+ - \text{Ni}) = 1.33 \pm 0.10\text{ eV}$. Rotational analysis of four bands has allowed the bond length of the ground state to be determined as $r_0 = 2.3211 \pm 0.0007\text{ \AA}$. These results have been compared to an analogous investigation of AlCu, which was presented in the preceding article.¹ It appears that there is little substantive difference in the chemical bonding in AlNi as compared to AlCu, at least for the neutral molecules.

Further work contemplated on this molecule includes dispersed fluorescence or stimulated emission studies to

probe the $3s^2_{\text{Al}}3d^9_{\text{Ni}}\sigma^2$ manifold of states, from which the ground $X^2\Delta_{5/2}$ state derives. Such studies would be very important in testing ligand field models of the electronic structure of intermetallic nickel-containing molecules.

ACKNOWLEDGMENTS

We thank Professor William H. Breckenridge for the use of the intracavity etalon employed in the high resolution studies and Jeff Bright for his expertise in preparing the AlNi alloy required for these studies. Research support from the National Science Foundation under Grant Nos. CHE-8912673 and CHE-9215193 is gratefully acknowledged. Acknowledgment is also made to the Eastman Kodak Company for a fellowship, and to the donors of the Petroleum Research Fund, administered by the American Chemical Society, for partial support of this research.

¹J. M. Behm, C. A. Arrington, J. D. Langenberg, and M. D. Morse, preceding paper, *J. Chem. Phys.* **99**, 6394 (1993).

²C. E. Moore, Atomic Energy Levels, Natl. Bur. Stand. U.S. Circ. No. 467 (U.S. G.P.O., Washington, D.C., 1971).

³Z.-W. Fu, and M. D. Morse, *J. Chem. Phys.* **90**, 3417 (1989).

⁴E. M. Spain and M. D. Morse, *J. Chem. Phys.* **97**, 4633 (1992).

⁵E. M. Spain and M. D. Morse, *J. Chem. Phys.* **97**, 4641 (1992).

⁶R. W. Field, *Ber. Bunsenges. Phys. Chem.* **86**, 771 (1982).

⁷S. Gerstenkorn and P. Luc, *Atlas du Spectre d'Absorption de la Molécule d'Iode* (CNRS, Paris, 1978); S. Gerstenkorn and P. Luc, *Rev. Phys. Appl.* **14**, 791 (1979).

⁸M. D. Morse, G. P. Hansen, P. R. R. Langridge-Smith, L.-S. Zheng, M. E. Geusic, D. L. Michalopoulos, and R. E. Smalley, *J. Chem. Phys.* **80**, 5400 (1984).

⁹E. M. Spain and M. D. Morse, *Int. J. Mass Spectrom. Ion Processes* **102**, 183 (1990).

¹⁰E. M. Spain and M. D. Morse, *J. Phys. Chem.* **96**, 2479 (1992).

¹¹L. M. Russon, S. A. Heidecke, M. K. Birke, J. Conceicao, P. B. Armentrout, and M. D. Morse, *Chem. Phys. Lett.* **204**, 2350 (1993).

¹²S. Taylor, E. M. Spain, and M. D. Morse, *J. Chem. Phys.* **92**, 2710 (1990).

- ¹³M. D. Morse, *Chemical Bonding in the Late Transition Metals: The Nickel and Copper Group Dimers*, in *Advances in Metal and Semiconductor Clusters*, Vol. I. *Spectroscopy and Dynamics*, edited by M. A. Duncan (JAI Press, Greenwich, Conn., 1993), p. 83.
- ¹⁴E. S. Chang, *J. Phys. Chem. Ref. Dat.* **19**, 119 (1990).
- ¹⁵C. Corliss and J. Sugar, *J. Phys. Chem. Ref. Data* **10**, 197 (1981).
- ¹⁶G. Herzberg, *Molecular Spectra and Molecular Structure I. Spectra of Diatomic Molecules*, 2nd ed. (Van Nostrand Reinhold, New York, 1950), p. 240.
- ¹⁷M. F. Cai, S. J. Tsay, T. P. Dzuga, K. Pak, and V. E. Bondybey, *J. Phys. Chem.* **94**, 1313 (1990).
- ¹⁸J. L. Elkind and P. B. Armentrout, *J. Phys. Chem.* **90**, 6576 (1986).
- ¹⁹R. Georgiadis, E. R. Fisher, and P. B. Armentrout, *J. Am. Chem. Soc.* **111**, 4251 (1989).
- ²⁰K. P. Huber and G. Herzberg, *Molecular Spectra and Molecular Structure. IV. Constants of Diatomic Molecules* (Van Nostrand Reinhold, New York, 1979).
- ²¹Z.-W. Fu, G. W. Lemire, G. A. Bishea, and M. D. Morse, *J. Chem. Phys.* **93**, 8420 (1990).